Antiangiogenic Arming of an Oncolytic Vaccinia Virus Enhances Antitumor Efficacy in Renal Cell Cancer Models[▽][†]

Kilian Guse,[1,2] Marta Sloniecka,[1,2] Iulia Diaconu,[1,2] Kathryn Ottolino-Perry,[3] Nan Tang,[3] Calvin Ng,[3] Fabrice Le Boeuf,[4] John C. Bell,[4] J. Andrea McCart,[3] Ari Ristimäki,[2‡] Sari Pesonen,[1,2] Vincenzo Cerullo,[1,2] and Akseli Hemminki[1,2]*

Cancer Gene Therapy Group, Molecular Cancer Biology Program, and Transplantation Laboratory, Haartman Institute, and Finnish Institute for Molecular Medicine, University of Helsinki, Helsinki, Finland[1]; HUSLAB, Helsinki University Central Hospital, Helsinki, Finland[2]; Toronto General Research Institute, Toronto, Canada[3]; and Centre for Cancer Therapeutics, Ottawa Health Research Institute, Ottawa, Canada[4]

Oncolytic vaccinia viruses have shown compelling results in preclinical cancer models and promising preliminary safety and antitumor activity in early clinical trials. However, to facilitate systemic application it would be useful to improve tumor targeting and antitumor efficacy further. Here we report the generation of vvdd-VEGFR-1-Ig, a targeted and armed oncolytic vaccinia virus. Tumor targeting was achieved by deletion of genes for thymidine kinase and vaccinia virus growth factor, which are necessary for replication in normal but not in cancer cells. Given the high vascularization typical with kidney cancers, we armed the virus with the soluble vascular endothelial growth factor (VEGF) receptor 1 protein for an antiangiogenic effect. Systemic application of high doses of vvdd-VEGFR-1-Ig resulted in cytokine induction in an immunocompromised mouse model. Upon histopathological analysis, splenic extramedullary hematopoiesis was seen in all virus-injected mice and was more pronounced in the vvdd-VEGFR-1-Ig group. Analysis of the innate immune response after intravenous virus injection revealed high transient and dose-dependent cytokine elevations. When medium and low doses were used for intratumoral or intravenous injection, vvdd-VEGFR-1-Ig exhibited a stronger antitumor effect than the unarmed control. Furthermore, expression of VEGFR-1-Ig was confirmed, and a concurrent antiangiogenic effect was seen. In an immunocompetent model, systemic vvdd-VEGFR-1-Ig exhibited superior antitumor efficacy compared to the unarmed control virus. In conclusion, the targeted and armed vvdd-VEGFR-1-Ig has promising anticancer activity in renal cell cancer models. Extramedullary hematopoiesis may be a sensitive indicator of vaccinia virus effects in mice.

In 2002 renal cell cancer accounted for more than 200,000 cases and 100,000 deaths worldwide (33). Unfortunately, chemotherapy, radiotherapy, and immunotherapy yield low response rates (9, 17) in this cancer type. Thus, prognosis for patients is poor, especially when the disease is metastatic, as median survival is only 8 months (19). Although recently approved drugs, such as sorafenib, sunitinib, temsirolimus, and bevacizumab, have provided additional tools for treatment of renal cell cancer (7), they are usually not curative, and thus new treatment approaches are needed.

Oncolytic vaccinia viruses are promising agents for cancer treatment and have shown compelling results in preclinical tumor models (40, 42, 45). Moreover, good safety and preliminary evidence of antitumor efficacy were seen in phase 1 clinical trials (22, 26, 32). Vaccinia virus has a strong oncolytic effect due to its fast replication cycle (45) and a high innate tropism to cancer tissue (34). Tumor targeting can be further improved by deleting vaccinia virus genes that are necessary for replication in normal cells but not in cancer cells. For example, deletions of either thymidine kinase (TK) or vaccinia virus growth factor (VGF) or both have been shown to reduce pathogenicity compared to wild-type virus (3, 5, 27). To enhance antitumor potency, oncolytic vaccinia viruses can be armed with therapeutic transgenes, such as immunostimulatory factors (26) or suicide genes (14, 16, 35). With regard to kidney cancer, an arming approach with antiangiogenenic molecules seems logical, considering the high vascularization characteristic of renal tumors (20).

Vascular endothelial growth factor (VEGF) is a major player in tumor angiogenesis and is highly expressed in renal cell cancers (29). VEGF binds to the fms-like-tyrosine kinase receptor (flt-1 or VEGFR-1) and kinase domain region receptor (KDR or VEGFR-2) with high affinity (13). The soluble vascular endothelial growth factor receptor 1-Ig fusion protein (VEGFR-1-Ig) used in this study is derived from the membrane-bound VEGFR-1 and binds human and murine VEGF without inducing vascular endothelial cell mitogenesis (31). Blocking VEGF with this or closely related molecules has been shown to inhibit tumor growth in several cancer models (18, 21, 25, 39).

Although tumor cell selective replication can be enhanced by deletion of TK and/or VGF to reduce pathogenicity (3, 5,

27), high doses of attenuated vaccinia virus may increase serum cytokine concentrations which parallel the onset of toxic events, as seen with other viral vectors (2, 38). The potential "early" toxicity associated with oncolytic vaccinia viruses has not been completely elucidated heretofore (36, 46).

Given the high vascularization of renal cell cancers and the pressing need to generate new antitumor agents with increased safety and efficacy, we hypothesized that an oncolytic vaccinia virus targeted by TK and VGF deletions and armed with VEGFR-1-Ig would exhibit enhanced antitumor efficacy due to its antiangiogenic properties in renal cell cancer models compared to a nonarmed control virus, allowing reduction of the treatment dose.

MATERIALS AND METHODS

Cell lines. Human clear cell renal cancer cell lines 786-O, ACHN, and 769-P were obtained from the American Type Culture Collection (Manassas, VA) and maintained under recommended conditions. Renca, a murine kidney cancer cell line, was a kind gift from A. Scarzello (National Cancer Institute, National Institutes of Health, Frederick, MD) and was cultured in RPMI medium supplemented with 10% fetal calf serum (FCS) and 1% L-glutamine and penicillin-streptomycin. Pooled human umbilical vein cells (HUVEC; Clonetics endothelial cell systems) were purchased from Lonza (Basel, Switzerland) and kept under the recommended conditions. Vero cells (African green monkey kidney epithelial cells) and CV-1 cells (African green monkey kidney fibroblasts) were obtained from the American Type Culture Collection and maintained under the recommended conditions.

Viruses. All vaccinia viruses used in this study are of the Western Reserve strain with disrupted TK and VGF genes for enhanced cancer cell specificity. For generation of vvdd-VEGFR-1-Ig, the luciferase gene was cloned into pSC65 (a kind gift from Bernie Moss, National Institutes of Health, Bethesda, MD) (6) under the control of the PE/L promoter, and *lacZ* (which is under the control of the P7.5 promoter) was replaced with *VEGFR-1-Ig* (VEGF receptor 1 fused to the Fc tail of human IgG antibody; kindly provided by K. Alitalo, University of Helsinki, Helsinki, Finland), resulting in pSC65-luc-VEGFR-1-Ig. This shuttle plasmid was cotransfected with vvdd-GFP (27) to CV-1 cells. Successfully recombined viruses, in which the luciferase gene and *VEGFR-1-Ig* replaced *GFP* in the TK locus, were selected by picking plaques that were positive for luciferase and negative for green fluorescent protein (GFP). Viruses were amplified on Vero cells and purified over a sucrose cushion, and titers were determined with a standard plaque assay on Vero cells as described previously (10). PFU virus titers (PFU/ml) determined by plaque assay have a certain variability and are estimates of the true number of viruses (8). The presence of the inserted genes was verified by PCR, and the expression of VEGFR-1-Ig by vvdd-VEGFR-1-Ig-infected cells was confirmed by Western blotting.

UV light inactivation of viruses was done as described before (44). Briefly, viruses were suspended in 10 μg/ml psoralen in Hanks balanced salt solution containing 0.1% bovine serum albumin. The suspension was incubated for 10 min at room temperature and then irradiated in a CL-1000 UV cross-linker (UVP, Cambridge, United Kingdom) with UV-A light (365 nm) for 3 min. A 5-day plaque assay was used to confirm lack of replication competent virus.

Marker gene transfer assay. Cells on 24-well plates were infected with different concentrations of virus suspended in growth medium containing 2% FCS. Thirty minutes later, cells were washed and incubated in complete growth medium for 4 h. Cells were lysed, and luciferase activity was measured according to the manufacturer's manual (luciferase assay system; Promega, Madison, WI).

in vitro **cytotoxicity assay.** Cells on 96-well plates were infected with different concentrations of virus suspended in growth medium containing 2% FCS. One hour later, cells were washed and incubated in growth medium containing 5% FCS for 72 h. Cell viability was then analyzed using MTS [3-(4,5-dimethylthiazol-2-yl)-5-(3-carboxymethoxyphenyl)-2-(4-sulfophenyl)-2H-tetrazolium] (Cell Titer 96 AQ$_{ueous}$ One Solution proliferation assay; Promega).

Animal experiments. Animal experiments were approved by the Experimental Animal Committee of the University of Helsinki and the Provincial Government of Southern Finland and the Animal Care Committee of the University Health Network, Ottawa, Canada.

Mice were purchased from Taconic (Ejby, Denmark, and Hudson, NY) at the age of 4 to 5 weeks and housed under standard conditions with food and water *ad libitum*.

For the immunodeficient models, 5×10^6 786-O cells were injected subcutaneously into flanks of nude Naval Medical Research Institute (NMRI) mice. When tumors reached the size of approximately 5 by 5 mm, virus was injected either intratumorally or intravenously. For bioluminescence imaging, mice were injected intraperitoneally with 4.5 mg of D-luciferin dissolved in phosphate-buffered saline (PBS), and after 10 min images were captured using the IVIS imaging series 100 system (Xenogen, Alameda, CA). VEGFR-1-Ig concentration in mouse serum was determined with a human IgG enzyme-linked immunosorbent assay (ELISA) kit (Immunology Consultants Laboratory, Newberg, OR).

For the immunocompetent model, 1×10^6 Renca cells were injected subcutaneously on shaved flanks of BALB/c mice. Virus was injected intravenously when tumors reached the size of approximately 5 by 5 mm. Imaging was done as described above.

To assess cytokine concentrations, mice were injected intravenously with virus, and blood samples were taken 6 h, 12 h, and 24 h postinjection. A fluorescence-activated cell sorting array with collected blood serum was performed for interleukin 6 (IL-6), tumor necrosis factor (TNF), monocyte chemoattractant protein 1 (MCP-1), gamma interferon (IFN-γ), macrophage inflammatory protein 1α (MIP-1α, or CCL3), KC (CXCL1), and regulated upon activation normal T-cell-expressed and secreted protein (RANTES; cytometric bead array mouse flex sets; BD Biosciences Pharmingen, Franklin Lakes, NJ).

Histopathology and immunofluorescence staining. Organs of animals were fixed in 10% neutral-buffered formalin. Following fixation, organs were trimmed, embedded in paraffin, sectioned (4 to 5 μm), stained with hematoxylin-eosin, and evaluated by a pathologist.

Four- to 5-μm cryosections of frozen tumors were prepared and fixed in acetone for 10 min at −20°C. Sections were incubated with normal donkey serum for 15 min and then reacted with primary polyclonal rabbit anti-von Willebrand factor (1:200 dilution; DakoCytomation, Denmark) overnight. After washing with PBS, sections were incubated with Alexa Fluor 488-labeled secondary antibody (1:250 dilution; Molecular Probes, Invitrogen, Carlsbad, CA) for 30 min. Sections were fixed in 4% paraformaldehyde and mounted with Vectashield mounting medium (Vector Laboratories, Burlingame, CA). Representative pictures of areas of the tumors with the highest microvessel density were captured at 20× magnification.

Statistical analysis. Tumor sizes as a function of time were compared by Mann-Whitney test (SPSS 16.0; SPSS Inc., Chicago, IL), and P values of <0.05 were considered statistically significant. A single preplanned comparison of mean tumor volume was done by using a two-tailed t test.

RESULTS

Virus constructs and *in vitro* gene transfer efficiency. All viruses used in the study are based on Western Reserve vaccinia viruses featuring deletions in the thymidine kinase and vaccinia growth factor genes for improved cancer cell selective replication (27). vvdd-GFP expresses GFP and guanine-hypoxanthine phosphoribosyltransferase (GPT) from the disrupted TK locus, while vvdd-luc expresses luciferase and LacZ from the same locus (Fig. 1A). To generate vvdd-VEGFR-1-Ig, the GFP-gpt cassette in vvdd-GFP was replaced with the genes for luciferase and VEGFR-1-Ig by homologous recombination. Transgenes were driven by vaccinia virus P7.5 or the synthetic PE/L (6) promoters.

In order to assess the transduction efficiency of the newly generated virus, human and mouse cell lines were infected and luciferase expression was assayed 4 h after infection. vvdd-luc and vvdd-GFP were used as positive and negative controls, respectively.

Human (786-O, ACHN, and 769-P) and murine (RENCA) renal cancer cells showed high luciferase expression (Fig. 1B and C; see also Fig. S1A and B in the supplemental material), while expression from infected HUVECs was 10- to 100-fold lower (Fig. 1D). vvdd-luc infection resulted in 10- to 20-fold-higher luciferase activity than infection with vvdd-VEGFR-1-Ig with all cell lines. UV inactivation of the viruses resulted in only approximately 10-fold-lower luciferase expression than
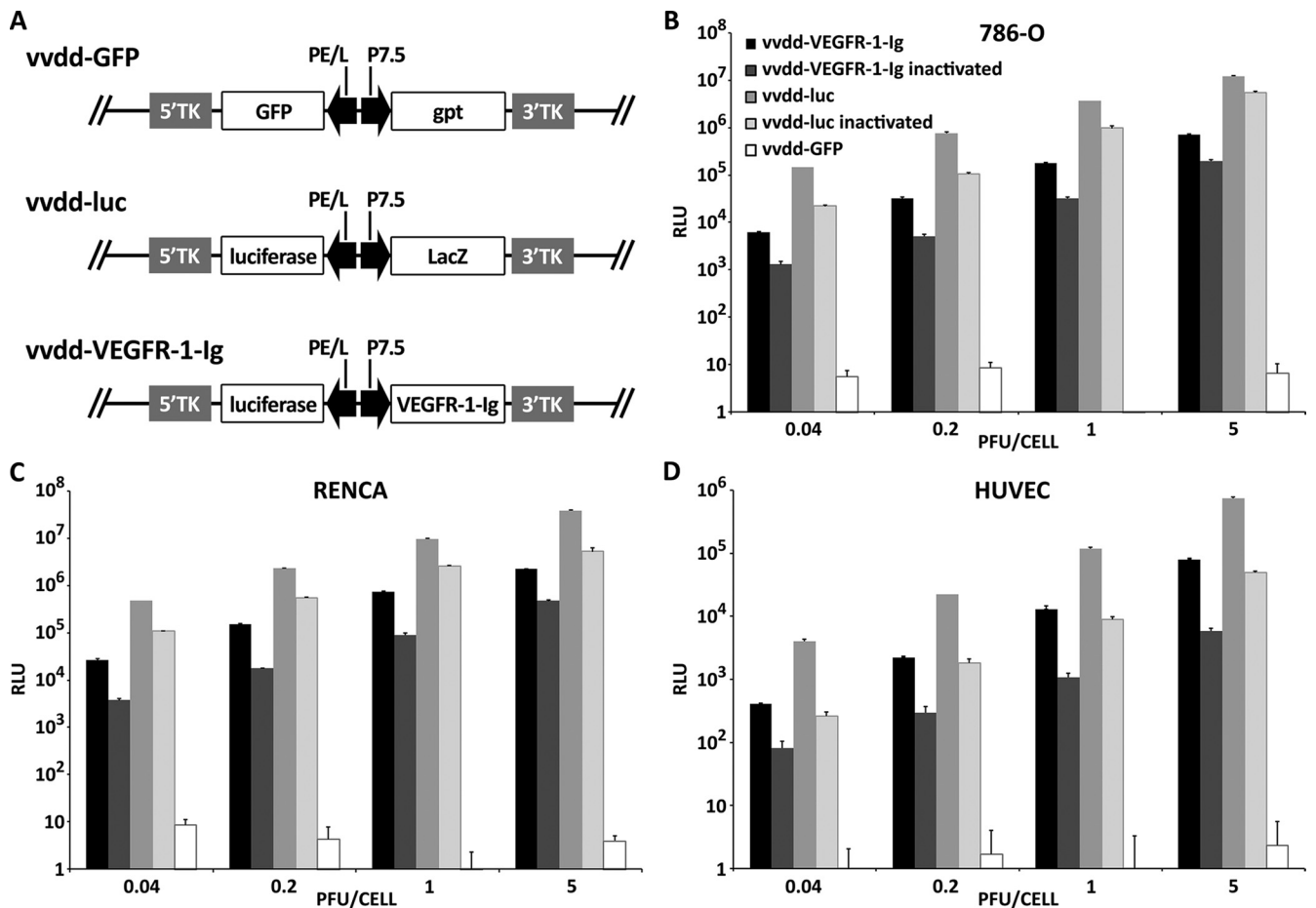
FIG. 1. Virus constructs and *in vitro* gene transfer efficiency. (A) Linear diagram of vaccinia virus constructs used in the study. vvdd-GFP has *GFP* and guanine-hypoxanthine phosphoribosyltransferase (*gpt*) in the TK locus, while vvdd-luc features *luc* and *lacZ* at this position. In vvdd-VEGFR-1-Ig, the *GFP-gpt* expression cassette of vvdd-GFP was replaced with *luc* and *VEGFR-1-Ig*. Transgenes are driven by vaccinia virus P7.5 and synthetic PE/L promoters. Human renal cancer cells (786-O) (B), murine renal cancer cells (Renca) (C), and HUVEC (D) were infected with different concentrations of replication-competent or UV-inactivated vaccinia viruses. HUVECs express 100-fold less luciferase than tumor cells. Luciferase expression was measured 4 h postinfection. vvdd-GFP does not express luciferase. Bars indicate standard errors. RLU, relative light units.

with respective noninactivated viruses, suggesting activity of the PE/L promoter even in the absence of replication.

vvdd-VEGFR-1-Ig retains oncolytic potency *in vitro*. To ensure that VEGFR-1-Ig arming did not impair the oncolytic effect, we infected different cell lines with vvdd-VEGFR-1-Ig, vvdd-luc, and vvdd-GFP and assayed cell viability. vvdd-VEGFR-1-Ig, vvdd-luc, and vvdd-GFP had similar oncolytic effects on 786-O, ACHN, and 769-P cells, resulting in complete cell killing after 3 days at a dose of 1 PFU/cell (Fig. 2A; see also Fig. S2A and B in the supplemental material). vvdd-VEGFR-1-Ig appeared to have a stronger oncolytic effect on Renca and HUVEC cells at low concentrations, while vvdd-luc and vvdd-GFP were equally oncolytic (Fig. 2B and C). However, these cells were also completely killed with all viruses 3 days after infection at 1 PFU/cell. Inactivated vvdd-luc and vvdd-GFP did not show any oncolytic effect, while infection with inactivated vvdd-VEGFR-1-Ig resulted in slightly reduced cell viability of all cell lines.

High-dose (10^7 PFU) virus application in an immunodeficient mouse model. Nude mice bearing subcutaneous 786-O

renal cell cancer tumors were injected intratumorally or intravenously with 10^7 PFU of vaccinia viruses or received mock treatment. Intratumoral virus application resulted in deaths of all three mice injected with vvdd-VEGFR-1-Ig and of one vvdd-luc-injected mouse over the first 9 days. Therefore, the tumor volume of the vvdd-VEGFR-1-Ig group could only be followed until day 9 (Fig. 3A). Mock-injected tumors grew rapidly, and therefore all mice had to be euthanized on day 19, while mean tumor volume decreased similarly in the vvdd-VEGFR-1-Ig and vvdd-luc groups ($P = 0.003$ and <0.001 compared to mock treatment; significant difference from day 7 on). In the virus-injected groups, bioluminescence imaging demonstrated strong expression coming from the tumors (see Fig. S3A in the supplemental material). However, especially from day 7 onwards, a widely disseminated luciferase signal was seen.

In parallel with intratumoral injection, intravenously administered virus resulted in death of the entire vvdd-VEGFR-1-Ig group within 9 days. vvdd-VEGFR-1-Ig was able to reduce average tumor size by 40% ($P = 0.002$ compared to mock
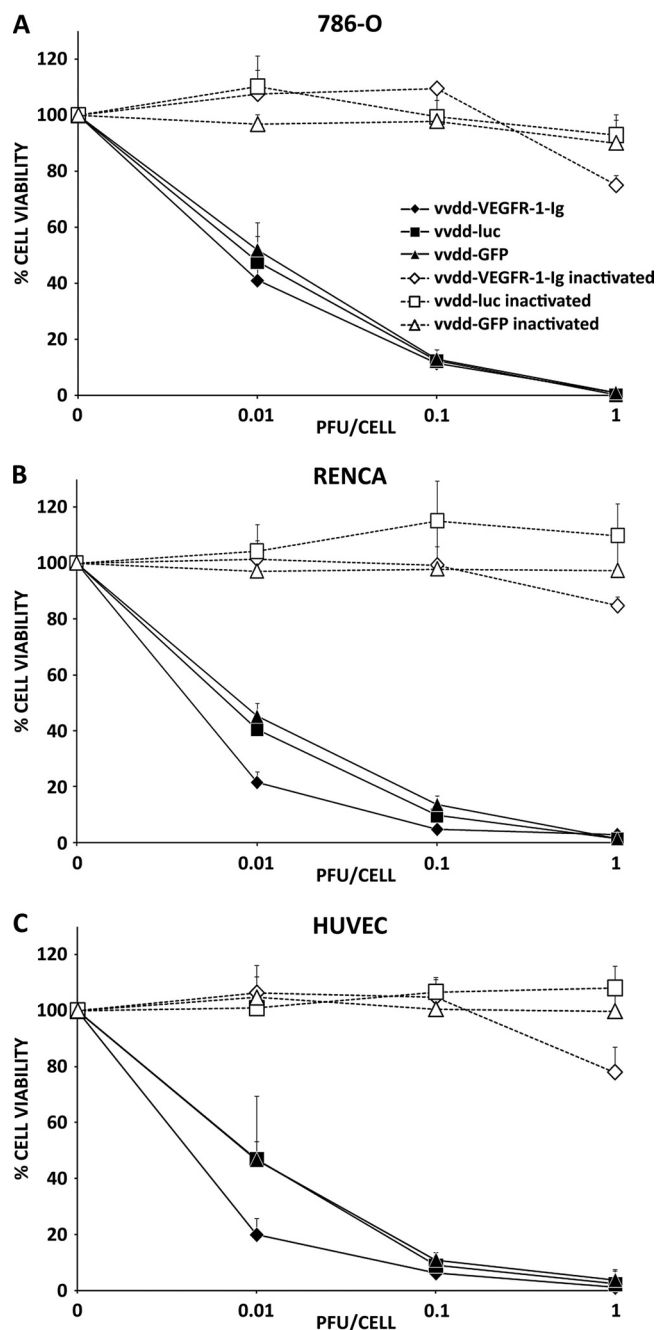
FIG. 2. *In vitro* oncolytic potency. Human renal cancer cells (786-O) (A), murine renal cancer cells (Renca) (B), and HUVEC (C) were infected with different concentrations of replication-competent or UV-inactivated vaccinia viruses. Three days later, cell viability was measured using an MTS assay. Bars indicate the standard errors.

into tumor-bearing and non-tumor-bearing mice. In this experiment only one mouse in the vvdd-VEFGR-1-Ig tumor-bearing group died. Hematoxylin-eosin-stained sections of liver, heart, kidney, and lung tissues revealed no histopathologic abnormalities. Spleens of all vvdd-VEGFR-1-Ig-injected mice showed signs of extramedullary hematopoiesis. The same was also found in the vvdd-luc group, although to a lesser extent, but was absent in the mock treatment group (Fig. 3C). Mice injected with virus displayed temporary elevation of cytokines MCP-1, IFN-γ, RANTES, KC, and MIP-1α (Fig. 3D). Tumor-bearing mice injected with vvdd-VEGFR-1-Ig showed increasing VEGFR-1-Ig serum levels over 3 days (Fig. 3E). However, the non-tumor-bearing vvdd-VEGFR-1-Ig-injected mice showed only low serum VEGFR-1-Ig concentrations, while VEGFR-1-Ig could not be detected in the vvdd-luc and mock-treated groups.
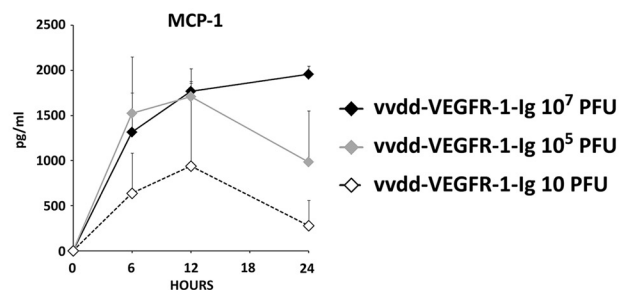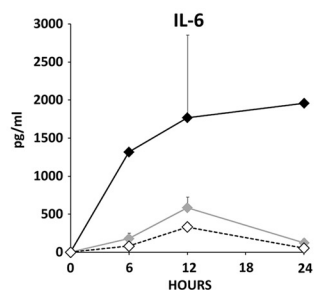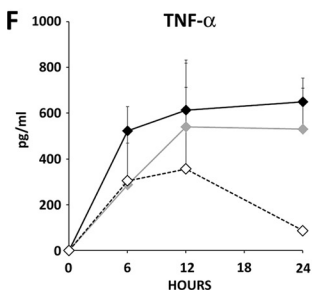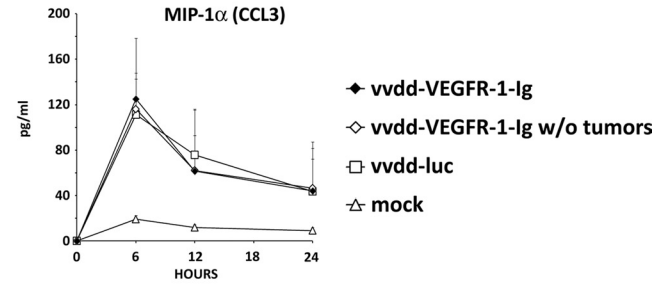
To determine a dose likely to be safe with regard to the acute inflammatory response, we sought to examine the innate immune response following intravenous administration of vvdd-VEGFR-1-Ig at different concentrations. A dose of 10^7 PFU resulted in strong induction of TNF-α, IL-6, and MCP-1 cytokines over 24 h (Fig. 3F). However, injection of 10^5 or 10 PFU of vvdd-VEGFR-1-Ig resulted in marked reductions in cytokine concentrations, especially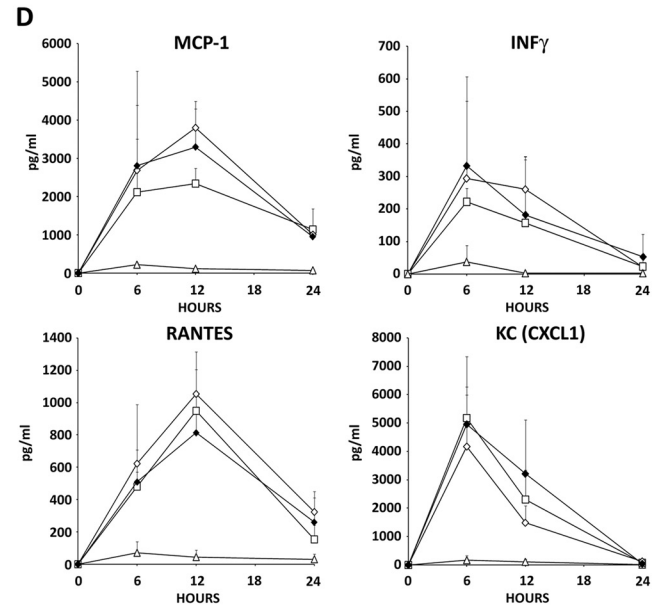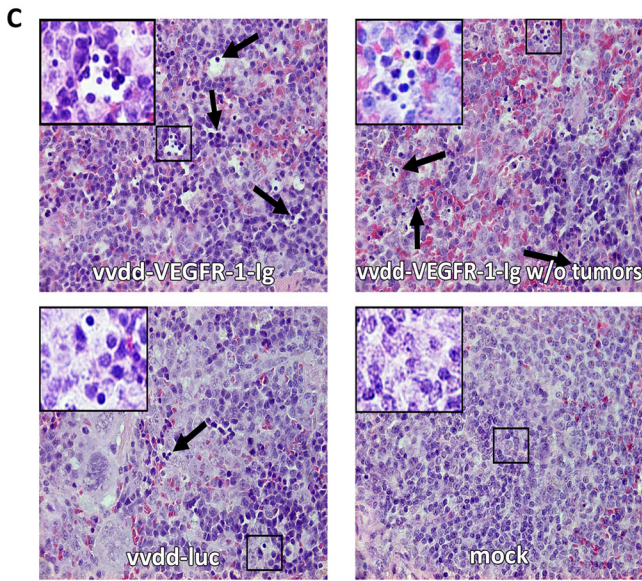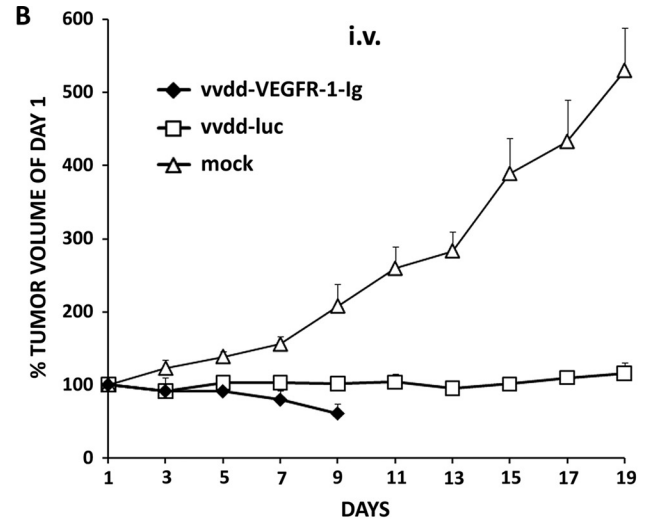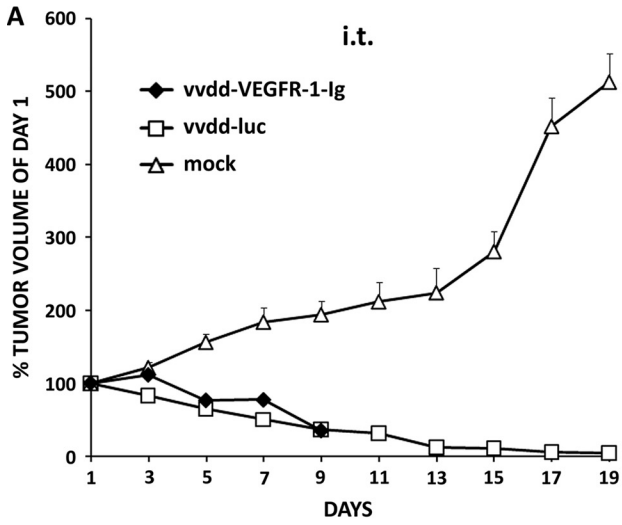 with regard to IL-6. Cytokine levels peaked at 12 h in mice injected with 10^5 and 10 PFU, while peak concentrations of mice injected with 10^7 PFU were not reached in the first 24 h.

Low (10 PFU) and medium (10^5 PFU) doses of vvdd-VEGFR-1-Ig result in reduced tumor vascularity and regression of tumors in an immunodeficient mouse model. When nude mice with subcutaneous 786-O kidney cancer tumors were injected intratumorally (i.t.) or intravenously with 10^5 or 10 PFU, none of the mice died. Intratumoral application of 5×10^4 PFU per tumor of vvdd-VEGFR-1-Ig and vvdd-luc resulted in efficient tumor size reduction, while mock-injected tumors grew rapidly ($P < 0.001$ for both virus groups compared to mock treatment) (Fig. 4A). Tumor progression was inhibited by 5 PFU of vvdd-luc administered i.t., but eventually the effect was lost and the tumors started to grow again. Impressively, injection of only 5 PFU of vvdd-VEGFR-1-Ig i.t. exhibited a strong antitumor effect ($P < 0.001$ compared to mock), similar to 5×10^4 PFU of vvdd-VEGFR-1-Ig or vvdd-luc.

With the medium dose (5×10^4 PFU), bioluminescence imaging showed localized luciferase expression from most tumors with both viruses on day 5 (see Fig. S4A in the supplemental material). Mice injected with low doses (5 PFU) showed expression in some tumors on day 5. Luciferase signals from vvdd-VEGFR-1-Ig-injected tumors were mostly lost by day 13, although some tumors injected with vvdd-luc continued to show expression.

Intravenous application of 10 PFU of vvdd-VEGFR-1-Ig and vvdd-luc did not significantly inhibit tumor growth (Fig. 4B). The same was seen with 10^5 PFU of vvdd-luc. However, intravenous vvdd-VEGFR-1-Ig at a dose of 10^5 PFU was able to reduce average tumor size to about 50% of the initial size ($P < 0.001$ compared to mock treatment). Bioluminescence imaging showed localized luciferase expression from two of six tumors of mice injected with 10^5 PFU vvdd-VEGFR-1-Ig, while in mice injected with the low dose (10 PFU) no expres-

treatment; significant difference from day 7 on), while vvdd-luc only abrogated tumor growth ($P = 0.001$ compared to mock treatment; significant difference from day 7 on) (Fig. 3B). Imaging of these mice showed a widely disseminated expression pattern in most mice (see Fig. S3B in the supplemental material).

The experiment was repeated, and organs were collected on day 3.Virus was injected intravenously at a dose of 10^7 PFU
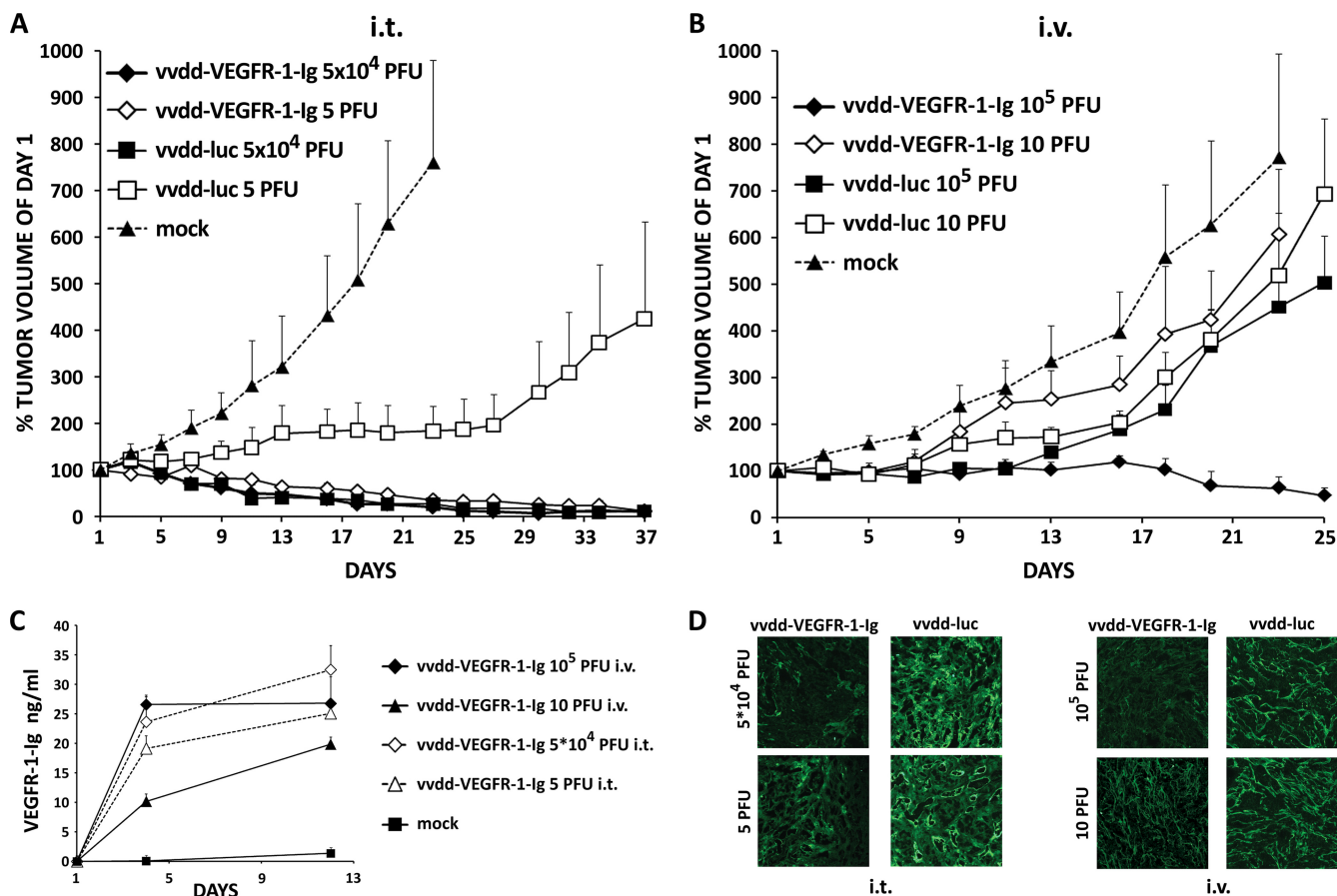
FIG. 4. Antitumor efficacy of 10^5 PFU and 10 PFU of antiangiogenic vaccinia virus in a nude mouse model. (A) Doses of 5×10^4 or 5 PFU of vaccinia virus were injected intratumorally into subcutaneous 786-O tumors in nude mice (three mice per group; two tumors per mouse), and tumor size was plotted relative to the size before virus injection on day 1. (B) In another experiment nude mice (three mice per group; two tumors per mouse) were intravenously injected with 10^5 or 10 PFU of vaccinia virus, and tumor volumes were followed. (C) VEGFR-1-Ig concentration was measured in the blood of treated mice. (D) At the end of the experiment tumors were collected, sections were made and stained with polyclonal von Willebrand factor antibody for blood vessels (green), and pictures of representative areas showing the highest blood vessel densities were taken at 20× magnification. Bars indicate standard errors.

sion was seen (see Fig. S4B). Similar imaging results were obtained with vvdd-luc.

Dose-dependent VEGFR-1-Ig expression was seen in the blood of the mice over 12 days (Fig. 4C). Furthermore, we found reduced blood vessel density in tumors treated with vvdd-VEGFR-1-Ig in comparison to vvdd-luc (Fig. 4D).

Systemic administration of high-dose (10^7 PFU) vvdd-VEGFR-1-Ig results in antitumor efficacy in an immunocompetent mouse model. BALB/c mice bearing subcutaneous mu-

rine Renca kidney cancer tumors were injected intravenously with 10^7 PFU of replicating or UV-inactivated vaccinia virus. Tumors of mock-injected mice grew rapidly, and all mice had to be euthanized on day 9 (Fig. 5A). In contrast, replicating vvdd-VEGFR-1-Ig and vvdd-luc showed equally strong antitumor effects, resulting in average tumor sizes of about 50% of the initial size ($P < 0.001$ for both groups compared to mock treatment). Inactivated vvdd-luc did not have any significant effect on tumor growth ($P = 0.232$ compared to the mock-

FIG. 3. Antitumor efficacy of 10^7 PFU of antiangiogenic vaccinia virus in a nude mouse model. Subcutaneous 786-O tumors in nude mice (three mice per group; two tumors per mouse) were injected i.t. with 5×10^6 PFU of vaccinia virus. (A) Tumor size was followed and plotted relative to the size before virus injection on day 1. All mice in the vvdd-VEGFR-1-Ig group were dead by day 9. (B) In another experiment nude mice were intravenously (i.v.) injected with 10^7 PFU of vaccinia viruses, and tumor volumes were plotted relative to initial size. In the vvdd-VEGFR-1-Ig group, all mice were dead by day 9. (C) An additional four nude mice per group with or without tumors were injected intravenously with 10^7 PFU of vvdd-VEGFR-1-Ig or vvdd-luc, and organs were harvested and hematoxylin-eosin stained after 3 days. Spleens of all virus-injected mice showed accumulations of small round-shaped, dark blue-stained cells, indicating extramedullary hematopoiesis. Large pictures are at 40× magnification, and small pictures in the upper left corner are at 63× magnification. Arrows indicate additional sites of extramedullary hematopoiesis. (D) Serum cytokine concentrations for MCP-1, IFN-γ, RANTES, KC, and MIP-1α were measured at the indicated time points. (E) VEGFR-1-Ig concentrations in serum of mice was assessed by ELISA. (F) Concentrations of TNF-α, IL-6, and MCP-1 were measured in serum of an additional three mice per group that were injected intravenously with different concentrations of vvdd-VEGFR-1-Ig. Bars indicate standard errors.

862
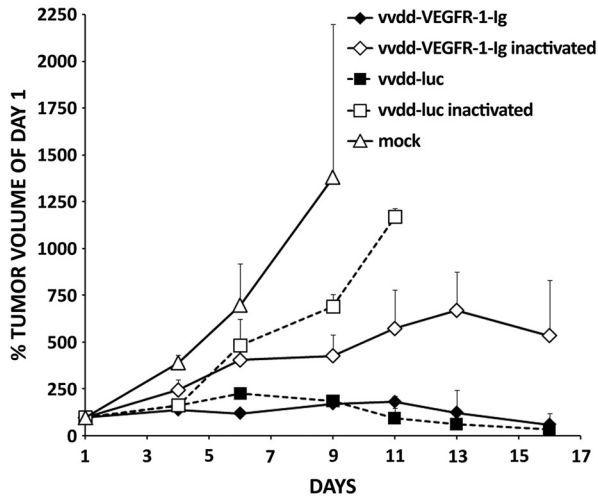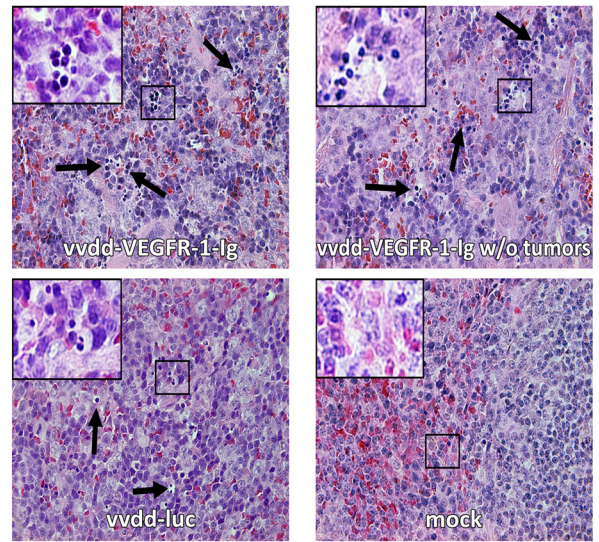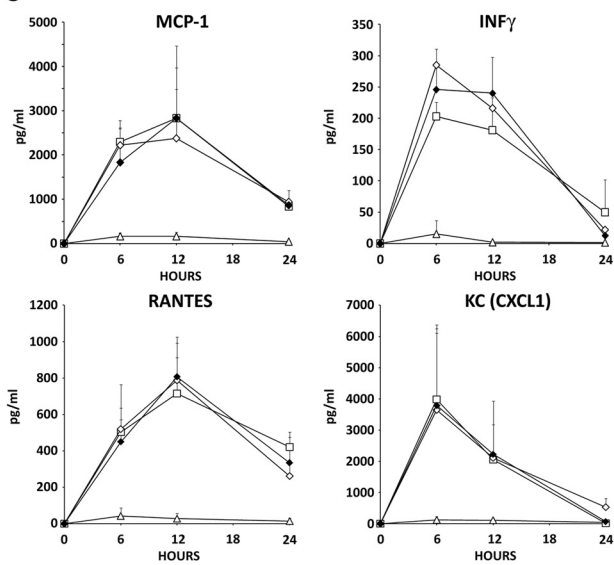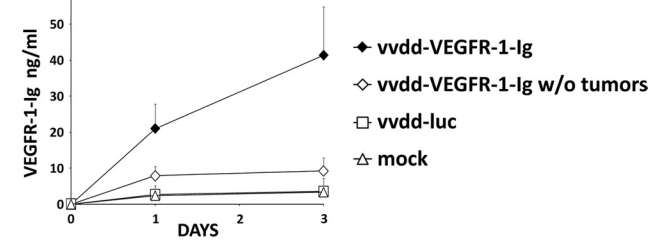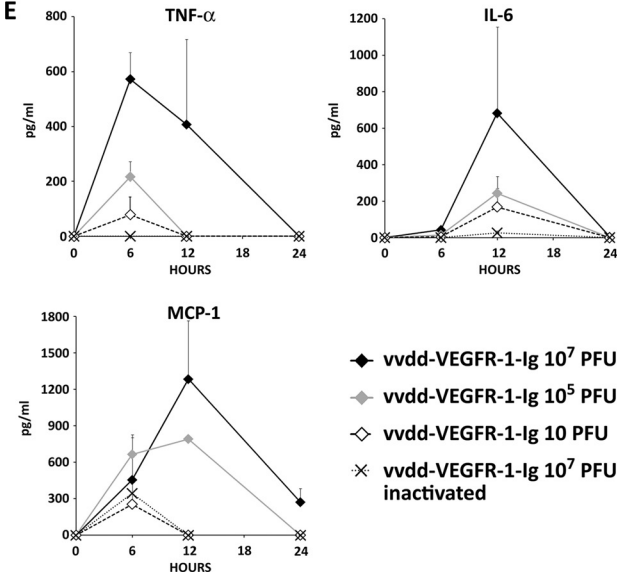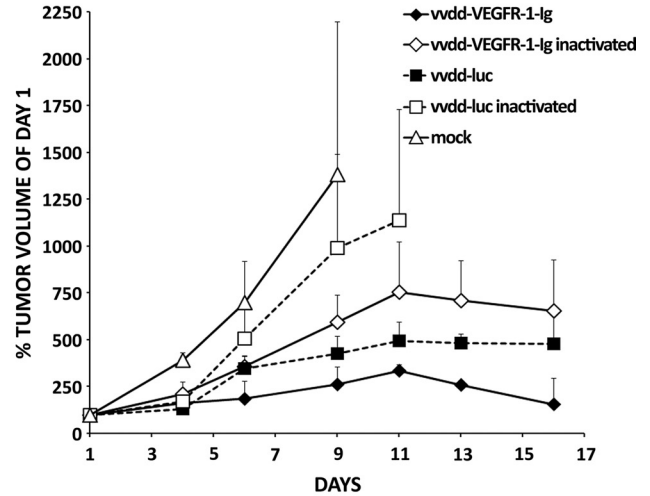
treated group on day 9), whereas inactivated vvdd-VEGFR-1-Ig was able to inhibit tumor progression in this aggressive cancer model ($P = 0.04$ compared to the mock-treated group on day 9).

Mice injected with replicating viruses showed luciferase expression coming mainly from tumors but also from elsewhere (see Fig. S5A in the supplemental material). In mice injected with inactivated viruses, tumors did not express detectable levels of luciferase, but strong signals were detected from the region of the lungs and/or liver. To confirm this finding, imaging of inactivated viruses was also performed at an earlier time point (2 days), and again luciferase expression was seen in lungs and/or liver (see Fig. S6 in the supplemental material).

We repeated the experiment and also included a non-tumor-bearing group. Hematoxylin-eosin-stained sections of organs collected on day 3 revealed no abnormalities of liver, heart, kidney, and lung tissues. Confirming the nude mouse data, spleens of all vvdd-VEGFR-1-Ig-injected mice showed signs of extramedullary hematopoiesis, which was seen to a lower extent also in vvdd-luc-injected mice but not in the mock treatment group (Fig. 5B). Analysis of the cytokine markers MCP-1, IFN-γ, RANTES, KC, and MIP-1α revealed temporary elevations after injection of vvdd-VEGFR-1-Ig and vvdd-luc (Fig. 5C). An increasing concentration of VEGFR-1-Ig was detected in tumor-bearing mice injected with vvdd-VEGFR-1-Ig, while tumor-free mice showed low expression levels (Fig. 5D).

To find a safe dose with regard to the acute inflammatory response, we analyzed the cytokine concentrations after intravenous administration of different concentrations of replicating or inactivated vvdd-VEFGR-1-Ig. Serum concentrations of TNF-α, IL-6, and MCP-1 peaked between 6 and 12 h in mice injected with 10^7 PFU of replicating virus (Fig. 5E), while mice injected with 10^5 and 10 PFU had a less pronounced cytokine response. Inactivated virus resulted in almost no elevation of TNF-α or IL-6, while MCP-1 was increased at 6 h.

Systemic administration of a medium dose (10^5 PFU) of vvdd-VEGFR-1-Ig results in antitumor efficacy with a reduced cytokine response in an immunocompetent mouse model. Mice with syngeneic Renca tumors were injected intravenously with 10^5 PFU of replicating or inactivated virus. Replicating vvdd-luc exhibited a strong antitumor effect, but vvdd-VEGFR-1-Ig was significantly more effective ($P < 0.001$ compared to mock treatment; $P = 0.002$ compared to vvdd-luc) (Fig. 5F). Tumors of mice injected with inactivated vvdd-luc grew almost as rapidly as tumors in the mock treatment group ($P = 0.184$ compared to mock treatment on day 9), whereas inactivated vvdd-VEGFR-1-Ig significantly inhibited tumor progression ($P = 0.043$ compared to mock treatment on day 9). Localized luciferase expression from the tumors was only seen in one of the vvdd-VEGFR-1-Ig-injected mice, while vvdd-luc-injected mice showed stronger and more disseminated expression (see Fig. S5B in the supplemental material). Mice injected with inactivated viruses did not show detectable luciferase expression.

DISCUSSION

Engineered oncolytic vaccinia viruses have demonstrated promising results in the treatment of cancer in preclinical models and early clinical trials (22, 26, 32, 40, 42, 45). However, most patients have not been cured, and thus the efficacy of the approach would benefit from further improvement. We generated vvdd-VEGFR-1-Ig, a targeted and armed oncolytic vaccinia virus designed to enhance oncolysis and reduce tumor angiogenesis for improved anticancer efficacy. To our knowledge, this is the first time that an antiangiogenic oncolytic vaccinia virus has been developed for and evaluated in kidney cancer models.

vvdd-VEGFR-1-Ig showed efficient transduction (Fig. 1; see also Fig. S1 in the supplemental material) and a strong oncolytic effect *in vitro* (Fig. 2; see also Fig. S2). In an immunocompromised mouse model, high-dose (10^7 PFU) application of the unarmed control virus vvdd-luc resulted in tumor eradication after intratumoral injection (Fig. 3A) and in tumor growth arrest after intravenous application (Fig. 3B). We hypothesized that a possible reason for mice dying in the vvdd-VEGFR-1-Ig group might have been high levels of the VEGF-inhibiting transgene product, as VEGF inhibition has been shown to harbor the potential for damage to the liver, kidneys, and vascular system (24, 41). However, histopathologic analysis of organs did not reveal tissue damage in livers or kidneys in mice injected with vvdd-VEGFR-1-Ig (Fig. 3C). Instead, extramedullary hematopoiesis in the spleen was found in vvdd-VEGFR-1-Ig-injected tumor-bearing and tumor-free animals. Also, mice injected with vvdd-luc showed splenic extramedullary hematopoiesis, although to a lesser extent, while it was not found in mock-injected mice. Thus, it seems that vaccinia virus itself can cause splenic extramedullary hematopoiesis, and this is further increased by VEGFR-1-Ig. Another possibility is decreased oxygenation due to infection of vascular elements and/or increased VEGFR-1-Ig levels. Splenic extramedullary hematopoiesis has been described after infection with other viruses, such as cytomegalovirus, herpes simplex virus, dengue

FIG. 5. Antitumor efficacy of 10^7 and 10^5 PFU of an antiangiogenic vaccinia virus in an immunocompetent mouse model. (A) BALB/c mice bearing subcutaneous tumors (three mice per group; two tumors per mouse) induced with Renca cells were injected intravenously with 10^7 PFU of replicating or UV-inactivated vaccinia virus. Tumor size was followed and plotted relative to the size before virus injection on day 1. Note that all mice in the mock and vvdd-luc-inactivated groups had to be killed because of large tumors that formed by days 9 and 11, respectively. (B) An additional four tumor-bearing and tumor-free BALB/c mice per group were injected intravenously with 10^7 PFU of the indicated virus, and organs were harvested and hematoxylin-eosin stained 3 days later. Spleens of all virus-injected mice showed accumulations of small round-shaped, dark blue-stained cells, indicating extramedullary hematopoiesis. Large pictures are at 40× magnification, and small pictures in the upper left corner are at 63× magnification. Arrows indicate additional sites of extramedullary hematopoiesis. (C) Serum cytokine concentrations for MCP-1, IFN-γ, RANTES, KC, and MIP-1α were measured at the indicated time points. (D) VEGFR-1-Ig concentrations in serum of the mice were assessed by ELISA. (E) An additional three BALB/c mice per group were intravenously injected with different concentrations of replicating or inactivated vvdd-VEGFR-1-Ig, and TNF-α, IL-6, and MCP-1 serum levels were measured. (F) In another experiment, tumor-bearing BALB/c mice (three mice per group; two tumors per mouse) were intravenously injected with 10^5 PFU of replicating or inactivated vaccinia virus. Rapid tumor growth required killing of all mice in the mock-treated and vvdd-luc-inactivated groups by day 9 and 11, respectively. Bars indicate standard errors.

virus, and human immunodeficiency virus (1, 23), and hepatic extramedullary hematopoiesis has been seen with adenovirus (37), but neither has previously been reported for vaccinia virus. Formal toxicity studies would be needed to understand the safety/toxicity profile of the viruses used here.

Widely disseminated virus-mediated luciferase expression was seen (see Fig. S3 in the supplemental material), possibly originating from the skin, since vaccinia virus is known to have dermal tropism (4, 28). However, for the vaccinia viruses used here, luciferase expression is not linked to replication. Therefore, luciferase expression is indicative of biodistribution of the virus rather than of off-target replication. Tumor selective replication of TK- and VGF-deleted viruses (vvdd backbone) in nude mice has been confirmed before (27). In fact, when tumor-free mice were injected with vvdd-VEGFR-1-Ig, low VEGFR-1-Ig serum concentrations were observed, suggesting tumor selectivity of the virus (Fig. 3E). Since the transgene is not linked to replication, input virus is expected to produce VEGFR-1-Ig, but in the absence of virus replication only low levels result.

Because strong activation of innate immune sensors after high-dose application of vaccinia virus (36, 46) can be toxic, we assessed the levels of key cytokines following intravenous administration of 10^7 PFU. Temporary increases in MCP-1, IFN-γ, RANTES, KC, and MIP-1α were seen for all viruses, mostly returning to baseline after 24 h (Fig. 3D). To find a safe dose, as estimated by the cytokine response, additional mice were injected with high (10^7 PFU), medium (10^5 PFU), and low (10 PFU) doses. With the high dose, elevations of TNF-α, IL-6, and MCP-1 levels were observed, and values were still increasing at the last time point (24 h) analyzed (Fig. 3F). Although medium and low doses also resulted in an inflammatory response, cytokine levels were markedly lower, peaking already at 12 h and decreasing earlier than with the high dose. Because cytokine induction was dose dependent, and high cytokine levels may correlate with severe or even lethal toxicity in animals and humans treated with viral gene therapy (1, 33), it would be key to maintain low cytokine concentrations while retaining antitumor efficacy. Therefore, we performed another animal experiment with lower amounts of virus (10^5 and 10 PFU). In this experiment, none of the mice died or showed obvious signs of toxicity. Regardless of the route of administration, vvdd-VEGFR-1-Ig was more effective than vvdd-luc (Fig. 4A and B), which was probably caused by VEGFR-1-Ig-mediated inhibition of the vasculature (Fig. 3C and D).

Since the immune system may play an important role in determining the safety and efficacy of oncolytic virotherapy, immunocompetent models might be superior to immunodeficient systems in predicting patient outcomes. Therefore, we used an aggressive syngeneic mouse model of renal cell cancer, where we injected replicating and inactivated viruses intravenously. While high doses (10^7 PFU) of replicating vvdd-VEGFR-1-Ig and vvdd-luc were equally efficient in tumor size reduction, inactivated vvdd-VEGFR-1-Ig seemed to result in better tumor growth inhibition than inactivated vvdd-luc, suggesting antitumor efficacy of the transgene product VEGFR-1-Ig (Fig. 5A).

Luciferase expression mediated by the replicating viruses appeared to be more restricted to tumor tissue in the immunocompetent models than in the immunodeficient models (compare Fig. S5A and S3B in the supplemental material). This might be due to more rapid virus clearance in normal tissues of hosts with an intact immune system versus those from a partially immune-privileged tumor environment (30).

Surprisingly, and in contrast to data with replication-competent viruses, luciferase expression mediated by UV-inactivated, and therefore replication-defective, viruses seemed to come primarily from the liver and/or lungs (see Fig. S5A and S6 in the supplemental material). One possible reason for the difference could be that uptake of the imaging substrate D-luciferin might be increased in areas of virus replication. However, we speculate that replication competence results in enhanced tumor selectivity, as the virus multiplies in the tumor but not in normal tissues, therefore increasing the signal from the tumor (43). This, however, does not explain the smaller liver/lung signal seen in the mice injected with replication-competent virus. Perhaps as a clue, we found that a replication-competent vaccinia virus induces a stronger and faster innate immune response than a replication-deficient virus. Therefore, virus might be cleared more rapidly from normal organs in the presence of virus replication (in the tumor) than in the absence of virus replication (in the tumor). Taken together, faster clearance from normal tissues and concurrent amplification in tumors might explain the differences in biodistribution.

We also analyzed possible organ damage and cytokine levels in the immunocompetent Renca model. Extramedullary hematopoiesis in the spleen was found in vvdd-VEGFR-1-Ig-injected mice and to a lower extent in vvdd-luc-injected mice (Fig. 5B), as was the case in the immunodeficient model. Livers, kidneys, hearts, and lungs did not show any histopathologic changes. Further studies could include bone marrow and other organs. Temporary induction of the cytokine markers MCP-1, IFN-γ, RANTES, KC, and MIP-1α was seen, with levels mostly returning to baseline after 24 h (Fig. 5C). Compared to tumor-bearing mice, tumor-free animals injected with vvdd-VEGFR-1-Ig had only low serum levels of VEGFR-1-Ig, suggesting tumor-specific replication and transgene expression (Fig. 5D). In a dose range-finding experiment with vvdd-VEGFR-1-Ig, we observed less-pronounced cytokine responses than in the immunocompromised model, with values returning to baseline at 24 h (Fig. 5E). Lowering the dose from 10^7 PFU to 10^5 PFU resulted in a lower cytokine response. Further studies are needed to evaluate whether these viruses can cause toxicity.

To assess if antitumor efficacy could be retained with the less immunogenic dose, an additional three mice per group were injected with 10^5 PFU. We found that replicating vvdd-VEGFR-1-Ig performed significantly better than vvdd-luc ($P = 0.002$) (Fig. 5F). Also, inactivated vvdd-VEGFR-1-Ig significantly inhibited tumor growth while inactivated vvdd-luc did not have any effect.

In conclusion, we have described here the arming of an oncolytic vaccinia virus with an antiangiogenic molecule which resulted in improved antitumor efficacy in immunodeficient and immunocompetent murine kidney cancer models. Cytokine analysis underscored the importance of using an optimal virus dose to avoid innate immune reactions. Systemic delivery of moderate (10^5 PFU) doses of vvdd-VEGFR-1-Ig inhibited tumor growth significantly better than the unarmed control virus, confirming the rationale that the antiangiogenic arming

approach allows for lowering the virus dose while retaining antitumor efficacy.

These preclinical data facilitate clinical development of armed oncolytic vaccinia viruses for clinical trials in renal cell cancer patients. Since antiangiogenic therapies have recently been demonstrated to be useful for many other common tumor types, including colorectal, breast, lung, ovarian, pancreatic, and liver (11), it is unlikely that the utility of the approach described here would be restricted to renal cell cancer. However, because high concentrations of VEGF-inhibiting molecules have been shown to cause toxicity in mice (24, 41) and humans (12, 15, 47), additional regulatory elements for the VEGFR-1-Ig expression might be needed. Also, our findings suggest that extramedullary hematopoiesis might be a sensitive indicator of vaccinia virus effects in mice.

REFERENCES

1. **Adler, S. P., and B. Marshall.** 2007. Cytomegalovirus infections. Pediatr. Rev. **28:**92–100.
2. **Brunetti-Pierri, N., D. J. Palmer, A. L. Beaudet, K. D. Carey, M. Finegold, and P. Ng.** 2004. Acute toxicity after high-dose systemic injection of helper-dependent adenoviral vectors into nonhuman primates. Hum. Gene Ther. **15:**35–46.
3. **Buller, R. M., S. Chakrabarti, J. A. Cooper, D. R. Twardzik, and B. Moss.** 1988. Deletion of the vaccinia virus growth factor gene reduces virus virulence. J. Virol. **62:**866–874.
4. **Buller, R. M., and G. J. Palumbo.** 1991. Poxvirus pathogenesis. Microbiol. Rev. **55:**80–122.
5. **Buller, R. M., G. L. Smith, K. Cremer, A. L. Notkins, and B. Moss.** 1985. Decreased virulence of recombinant vaccinia virus expression vectors is associated with a thymidine kinase-negative phenotype. Nature **317:**813–815.
6. **Chakrabarti, S., J. R. Sisler, and B. Moss.** 1997. Compact, synthetic, vaccinia virus early/late promoter for protein expression. Biotechniques **23:**1094–1097.
7. **Chowdhury, S., J. M. Larkin, and M. E. Gore.** 2008. Recent advances in the treatment of renal cell carcinoma and the role of targeted therapies. Eur. J. Cancer **44:**2152–2161.
8. **Condit, R. C.** 2007. Principles of virology, p. 38–40. In D. M. Knipe and P. M. Howley (ed.), Fields virology, 5th ed., vol. 1. Lippincott Williams & Wilkins, Philadelphia, PA.
9. **Coppin, C., F. Porzsolt, A. Awa, J. Kumpf, A. Coldman, and T. Wilt.** 2005. Immunotherapy for advanced renal cell cancer. Cochrane Database Syst. Rev. **2005**(1):CD001425.
10. **Earl, P. L., B. Moss, L. S. Wyatt, and M. W. Carroll.** 1998. Preparation of cell cultures and vaccinia virus stocks, p. 16.17.1–16.17.19. Current protocols in molecular biology, vol. 2. Greene Publishing Associates and Wiley Interscience, New York, NY.
11. **Ellis, L. M., and D. J. Hicklin.** 2008. VEGF-targeted therapy: mechanisms of anti-tumour activity. Nat. Rev. Cancer **8:**579–591.
12. **Eskens, F. A., and J. Verweij.** 2006. The clinical toxicity profile of vascular endothelial growth factor (VEGF) and vascular endothelial growth factor receptor (VEGFR) targeting angiogenesis inhibitors a review. Eur. J. Cancer **42:**3127–3139.
13. **Ferrara, N.** 1999. Role of vascular endothelial growth factor in the regulation of angiogenesis. Kidney Int. **56:**794–814.
14. **Foloppe, J., J. Kintz, N. Futin, A. Findeli, P. Cordier, Y. Schlesinger, C. Hoffmann, C. Tosch, J. M. Balloul, and P. Erbs.** 2008. Targeted delivery of a suicide gene to human colorectal tumors by a conditionally replicating vaccinia virus. Gene Ther. **15:**1361–1371.
15. **George, B. A., X. J. Zhou, and R. Toto.** 2007. Nephrotic syndrome after bevacizumab: case report and literature review. Am. J. Kidney Dis. **49:**e23–e29.
16. **Gnant, M. F., M. Puhlmann, H. R. Alexander, Jr., and D. L. Bartlett.** 1999. Systemic administration of a recombinant vaccinia virus expressing the cytosine deaminase gene and subsequent treatment with 5-fluorocytosine leads to tumor-specific gene expression and prolongation of survival in mice. Cancer Res. **59:**3396–3403.
17. **Godley, P., and S. W. Kim.** 2002. Renal cell carcinoma. Curr. Opin. Oncol. **14:**280–285.
18. **Goldman, C. K., R. L. Kendall, G. Cabrera, L. Soroceanu, Y. Heike, G. Y. Gillespie, G. P. Siegal, X. Mao, A. J. Bett, W. R. Huckle, K. A. Thomas, and D. T. Curiel.** 1998. Paracrine expression of a native soluble vascular endothelial growth factor receptor inhibits tumor growth, metastasis, and mortality rate. Proc. Natl. Acad. Sci. U. S. A. **95:**8795–8800.
19. **Haviv, Y. S., W. J. van Houdt, B. Lu, D. T. Curiel, and Z. B. Zhu.** 2004. Transcriptional targeting in renal cancer cell lines via the human CXCR4 promoter. Mol. Cancer Ther. **3:**687–691.
20. **Kaelin, W. G., Jr.** 2004. The von Hippel-Lindau tumor suppressor gene and kidney cancer. Clin. Cancer Res. **10:**6290S–6295S.
21. **Kim, K. J., B. Li, J. Winer, M. Armanini, N. Gillett, H. S. Phillips, and N. Ferrara.** 1993. Inhibition of vascular endothelial growth factor-induced angiogenesis suppresses tumour growth in vivo. Nature **362:**841–844.
22. **Kirn, D. H., and S. H. Thorne.** 2009. Targeted and armed oncolytic poxviruses: a novel multi-mechanistic therapeutic class for cancer. Nat. Rev. Cancer **9:**64–71.
23. **Kolb-Maurer, A., and W. Goebel.** 2003. Susceptibility of hematopoietic stem cells to pathogens: role in virus/bacteria tropism and pathogenesis. FEMS Microbiol. Lett. **226:**203–207.
24. **Mahasreshti, P. J., M. Kataram, M. H. Wang, C. R. Stockard, W. E. Grizzle, D. Carey, G. P. Siegal, H. J. Haisma, R. D. Alvarez, and D. T. Curiel.** 2003. Intravenous delivery of adenovirus-mediated soluble FLT-1 results in liver toxicity. Clin. Cancer Res. **9:**2701–2710.
25. **Mahasreshti, P. J., J. G. Navarro, M. Kataram, M. H. Wang, D. Carey, G. P. Siegal, M. N. Barnes, D. M. Nettelbeck, R. D. Alvarez, A. Hemminki, and D. T. Curiel.** 2001. Adenovirus-mediated soluble FLT-1 gene therapy for ovarian carcinoma. Clin. Cancer Res. **7:**2057–2066.
26. **Mastrangelo, M. J., H. C. Maguire, Jr., L. C. Eisenlohr, C. E. Laughlin, C. E. Monken, P. A. McCue, A. J. Kovatich, and E. C. Lattime.** 1999. Intratumoral recombinant GM-CSF-encoding virus as gene therapy in patients with cutaneous melanoma. Cancer Gene Ther. **6:**409–422.
27. **McCart, J. A., J. M. Ward, J. Lee, Y. Hu, H. R. Alexander, S. K. Libutti, B. Moss, and D. L. Bartlett.** 2001. Systemic cancer therapy with a tumor-selective vaccinia virus mutant lacking thymidine kinase and vaccinia growth factor genes. Cancer Res. **61:**8751–8757.
28. **Naik, A. M., S. Chalikonda, J. A. McCart, H. Xu, Z. S. Guo, G. Langham, D. Gardner, S. Mocellin, A. E. Lokshin, B. Moss, H. R. Alexander, and D. L. Bartlett.** 2006. Intravenous and isolated limb perfusion delivery of wild type and a tumor-selective replicating mutant vaccinia virus in nonhuman primates. Hum. Gene Ther. **17:**31–45.
29. **Nicol, D., S. I. Hii, M. Walsh, B. Teh, L. Thompson, C. Kennett, and D. Gotley.** 1997. Vascular endothelial growth factor expression is increased in renal cell carcinoma. J. Urol. **157:**1482–1486.
30. **O'Connell, J., M. W. Bennett, G. C. O'Sullivan, J. K. Collins, and F. Shanahan.** 1999. Fas counter-attack: the best form of tumor defense? Nat. Med. **5:**267–268.
31. **Olofsson, B., E. Korpelainen, M. S. Pepper, S. J. Mandriota, K. Aase, V. Kumar, Y. Gunji, M. M. Jeltsch, M. Shibuya, K. Alitalo, and U. Eriksson.** 1998. Vascular endothelial growth factor B (VEGF-B) binds to VEGF receptor-1 and regulates plasminogen activator activity in endothelial cells. Proc. Natl. Acad. Sci. U. S. A. **95:**11709–11714.
32. **Park, B. H., T. Hwang, T. C. Liu, D. Y. Sze, J. S. Kim, H. C. Kwon, S. Y. Oh, S. Y. Han, J. H. Yoon, S. H. Hong, A. Moon, K. Speth, C. Park, Y. J. Ahn, M. Daneshmand, B. G. Rhee, H. M. Pinedo, J. C. Bell, and D. H. Kirn.** 2008. Use of a targeted oncolytic poxvirus, JX-594, in patients with refractory primary or metastatic liver cancer: a phase I trial. Lancet Oncol. **9:**533–542.
33. **Parkin, D. M., F. Bray, J. Ferlay, and P. Pisani.** 2005. Global cancer statistics, 2002. CA Cancer J. Clin. **55:**74–108.
34. **Peplinski, G. R., A. K. Tsung, M. J. Casey, J. B. Meko, T. N. Fredrickson, R. M. Buller, and J. A. Norton.** 1996. In vivo murine tumor gene delivery and expression by systemic recombinant vaccinia virus encoding interleukin-1beta. Cancer J. Sci. Am. **2:**21–27.
35. **Puhlmann, M., M. Gnant, C. K. Brown, H. R. Alexander, and D. L. Bartlett.** 1999. Thymidine kinase-deleted vaccinia virus expressing purine nucleoside phosphorylase as a vector for tumor-directed gene therapy. Hum. Gene Ther. **10:**649–657.
36. **Quigley, M., J. Martinez, X. Huang, and Y. Yang.** 2009. A critical role for

direct TLR2-MyD88 signaling in CD8 T cell clonal expansion and memory formation following vaccinia viral infection. Blood **113:**2256–2264.

37. **Raki, M., A. Kanerva, A. Ristimaki, R. A. Desmond, D. T. Chen, T. Ranki, M. Sarkioja, L. Kangasniemi, and A. Hemminki.** 2005. Combination of gemcitabine and Ad5/3-Δ24, a tropism modified conditionally replicating adenovirus, for the treatment of ovarian cancer. Gene Ther. **12:**1198–1205.

38. **Raper, S. E., N. Chirmule, F. S. Lee, N. A. Wivel, A. Bagg, G. P. Gao, J. M. Wilson, and M. L. Batshaw.** 2003. Fatal systemic inflammatory response syndrome in a ornithine transcarbamylase deficient patient following adenoviral gene transfer. Mol. Genet. Metab. **80:**148–158.

39. **Sallinen, H., M. Anttila, J. Narvainen, J. Koponen, K. Hamalainen, I. Kholova, T. Heikura, P. Toivanen, V. M. Kosma, S. Heinonen, K. Alitalo, and S. Yla-Herttuala.** 2009. Antiangiogenic gene therapy with soluble VEGFR-1, -2, and -3 reduces the growth of solid human ovarian carcinoma in mice. Mol. Ther. **17:**278–284.

40. **Shen, Y., and J. Nemunaitis.** 2005. Fighting cancer with vaccinia virus: teaching new tricks to an old dog. Mol. Ther. **11:**180–195.

41. **Sivanandam, V. G., S. L. Stephen, R. Hernandez-Alcoceba, P. Alzuguren, M. Zabala, N. van Rooijen, C. Qian, I. Berger, M. L. Gross, J. Prieto, and S. Kochanek.** 2008. Lethality in an anti-angiogenic tumor gene therapy model upon constitutive but not inducible expression of the soluble vascular endothelial growth factor receptor 1. J. Gene Med. **10:**1083–1091.

42. **Thorne, S. H., D. L. Bartlett, and D. H. Kirn.** 2005. The use of oncolytic vaccinia viruses in the treatment of cancer: a new role for an old ally? Curr. Gene Ther. **5:**429–443.

43. **Thorne, S. H., T. H. Hwang, W. E. O'Gorman, D. L. Bartlett, S. Sei, F. Kanji, C. Brown, J. Werier, J. H. Cho, D. E. Lee, Y. Wang, J. Bell, and D. H. Kirn.** 2007. Rational strain selection and engineering creates a broad-spectrum, systemically effective oncolytic poxvirus, JX-963. J. Clin. Investig. **117:**3350–3358.

44. **Tsung, K., J. H. Yim, W. Marti, R. M. Buller, and J. A. Norton.** 1996. Gene expression and cytopathic effect of vaccinia virus inactivated by psoralen and long-wave UV light. J. Virol. **70:**165–171.

45. **Zeh, H. J., and D. L. Bartlett.** 2002. Development of a replication-selective, oncolytic poxvirus for the treatment of human cancers. Cancer Gene Ther. **9:**1001–1012.

46. **Zhu, J., J. Martinez, X. Huang, and Y. Yang.** 2007. Innate immunity against vaccinia virus is mediated by TLR2 and requires TLR-independent production of IFN-beta. Blood **109:**619–625.

47. **Zhu, X., S. Wu, W. L. Dahut, and C. R. Parikh.** 2007. Risks of proteinuria and hypertension with bevacizumab, an antibody against vascular endothelial growth factor: systematic review and meta-analysis. Am. J. Kidney Dis. **49:**186–193.